ISSN: 0067-2904

Preparation, Characterization and Biological Evaluations of New Bis (Azo-Acen) Ligands and Some of their Divalent TM Complexes

Saad Madlool Mahdi
Department of Chemistry, College of Science, University of Babylon, Hilla, Iraq

Received: 6/11/2024 Accepted: 27/ 4/2025 Published: 30/3/2026

Abstract

A new azo-acetophenon ethylene-diamine ligands were synthesized through a multi-step procedure. The process initiated with the formation of an ACEN imine via that produced from the condensation of ethylene diamine and 4-aminoacetophenone, followed by diazotation of the ACEN amine group and subsequent coupling with components to form these two new ligands:- (1E,1'E)-N,N'-(ethane-1,2-diyl)bis(1-(4-((E)-(4,5-diphenyl-1H-imidazol-2-yl)diazenyl)phenyl)ethan-1-imine) L_1 and3,3'-((1E,1'E)-(((1E,1'E)-(ethane-1,2-diylbis(azanylylidene))bis(ethan-1-yl-1-ylidene)) bis(4,1-phenylene))bis(diazene-2,1-diyl))bis(naphthalen-2-ol) H_2L_2. Comprehensive characterization of these ligands was conducted using FTIR, NMR, UV-visible, and Mass Spectroscopy complemented by C.H.N analysis. The corresponding PtL_1 and pdL_2 complexes were synthesized and identified with the previously mentioned techniques, meanwhile another technique as molar conductivity, magnetic susceptibility and XRD diffraction to deduce their morphology and geometry, from the biological side, three effective parameters were studied for these complexes (antibacterial ZOI, antioxidant and MCF7 cell line).

Keywords: Azo Schiff, characterization, biological study, platinum complex, palladium complex, 4,5-diphenylimidazole ,2-naphthol.

تحضير وتشخيص وتقييم حيوي لليكاندات ثنائي (الازو–اسين) الجديدة وبعض من معقداتها للعناصر الانتقالية ثنائية الشحنة الموجبة

سعد مدلول مهدي
قسم الكيمياء, كلية العلوم, جامعة بابل, الحلة, العراق

الخلاصة

حضرت ليكاندي الازو–اسين (ازو قاعدة شف اسيتوفينون–اثيلين ثنائي الامين) الجديدة خلال عدة خطوات عملية ، ابتداء من تحضير قاعدة شف الاسين والناتجة من التفاعل التكثيفي للاسيتوفينون مع الاثيلين ثنائي الامين ، يتبعها ازوتة امين الاسين وازواجه مع نوعين من مكونات الازواج وهما (4،5–ثنائي فنيل اميدازول) لتحضير ليكاند الازو الاول و(2– نفثول) لتحضير ليكاند الازو الثاني ، حيث شخصت تلك الليكاندات الجديدة المحضرة بالعديد من الوسائل الطيفية (كطيف الاشعة تحت الحمراء وطيف الرنين النووي المغناطيسي و مطيافية الاشعة الفوق بنفسجية–المرئية و طيف تجزؤ الكتلة اضافة الى التحليل العناصري

*Email: sci.saad.madlool@uobabylon.edu.iq

الدقيق). وبالمقابل فقد حضرت معقدات (PtL_1) و (PdL_2) وشخصت بالوسائل الطيفية مسبوقة الذكر اضافة الى بقية التقنيات المتممة كالتوصيلية المولارية والحساسية المغناطيسية وحيود الاشعة السينية لاقرار شكل المعقدات وبناها الهندسية. تخللت الدراسة تقييما حيويا للمعقدات المحضرة، حيث قيست ثلاث من المؤشرات الحيوية المهمة كقياس التثبيط المضاد الحيوي ZOI ومضاد الاكسدة antioxidant اضافة الى دراسة خط سرطان الثدي MCF7.

1. Introduction

Azo compounds constitute a class of organic compounds distinguished by their nitrogen-nitrogen double bond (N=N) functional group [1]. These particular compounds are characterized by their vivid color spectra spanning yellow, red, and blue hues, [2]. These compounds are utilized as dyes and pigments in various industries, such as textiles [3], food [4] , and cosmetics [5].

Their synthesis typically involves coupling diazonium salt with a compound that contains a functional group capable of undergoing nucleophilic substitution, such as an amine or a phenol [6]. The resulting reaction produces an azo compound, which can be isolated and purified for use as a dye or pigment [7].

Azo-Imine compounds are a type of azo compound that contains an Imine as a ligand [8, 9]. These hybrid structures are synthesized through the coupling of Schiff base ligand with an azo compound, which results in the formation of an organic molecule with a nitrogen-nitrogen double bond (N=N) and nitrogen-carbon double bond (C=N) as a functional group.

The versatility of azo-imine compounds has spurred significant research into their catalytic applications, particularly in alcohol oxidation and olefin polymerization [10, 11]. Furthermore, these compounds have meticulously been scrutinized for their conceivable deployment as sensors [12] and molecular switches [13], primarily due to their remarkable aptitude to gracefully undergo reversibly metamorphic chromatic transformations when confronted with alterations in their immediate milieu.

In addition to their potential applications in chemistry and materials science, azo-imine compounds have also been investigated for their potential biological activities. Some studies have suggested that these compounds may have anticancer [14] and antimicrobial [15] properties, although more research is needed in these areas.

In material science, there are some applications of azo-imine compounds such, color colour-changing material [16], liquid crystal display and photo-responsive materials. Reversible color change can occur due to several different factors, including changes in temperature, pH, or the presence of certain chemicals or compounds. In some cases, reversible color change can be induced by exposure to light, such as in the case of photochromic or thermochromic materials [17].

Azo-Imine complexes have garnered significant attention for their potential applications across multiple fields. They have been explored as catalysts in many organic reactions [18] and as materials for optical devices. Additionally, the color changes and electronic properties of these complexes can make them useful in sensors and other optoelectronic devices [19]. Indeed, these complexes have an anticancer activity to some extent toward many cancer types [20-22] The distinctive characteristics and sensitivity of azo Imine complexes depend on the selection of metal, the properties of the ligands, and the structural features of the complexes [23]. The present study aims to synthesise new azo-imine ligands and their platinum and

palladium ions complexes, exploring their diverse biological applications to advance their potential role in combating various diseases.

2. Experimental Section

2.1 Materials and Methods

All chemical materials and organic solvents were commercially. FTIR spectra were obtained by using FTIR- ATR, Bruker ALPHA FTIR, and Elemental analysis (C.H.N.S) were recorded using EuRo VECTOR elemental analyzer. Bruker spectrometer (500 MHz for ^{1}H NMR and 125 MHz for ^{13}C-NMR, respectively) using a DMSO solvent, pH measurements were recorded by utilising pH meter model WTW 315i, electrical molar conductivity was measured at room temperature in DMF on WTW Inof Lab Cond 720 conductivity meter. UV- Visible spectra were obtained by UV_6100PC double beam spectrophotometer (200-700) nm and this instrumental limitation prevented the electronic spectroscopy for studied, EMC LAB, while in mass spectrometry an MSD Direct probe using ACQ method low energy M and using the ESI-MS technique for their complexes. Shimadzu 6300 AA spectrophotometer was used for metal ion in complexes determination, Auto Magnetic susceptibility Balance, and Sherwood was used for magnetic susceptibility measurements.

2.1.1 Imine Synthesis (ACEN) (N1E, N2E)-N1, N2-bis(1-(4-aminophenyl) ethylidene) ethane-1,2-diamine

ACEN was prepared by the modification of the procedure of Vogel's literature [24]. In a 500ml round bottom flask, the reaction mixture containing solvation of (20mmole, 2.7 gm) of p-amino acetophenone and ethylene diamine (10mmole, 0.66 gm) in 100 ml of hot ethanol. To catalyze the reaction, three drops of glacial acetic acid were added dropwise. The mixture was refluxed for 6 hours, and the reaction was monitored with the TLC technique. After refluxing, the reaction mixture was cooled in an ice bath, the Imine was developed, which then filtered and recrystallized with hot ethanol and dried, ACEN was A yellow solid Imine, chemical formula $C_{18}H_{22}N_4$; 83% yield; M.P. 111º-113º; (TLC, ethyl acetate: n-hexane 3:2, Rf : 0.83) ; FTIR data (cm^{-1}): 3248,3166 (NH_2 str.), 2995 (Ar-H),2960, 2913 (C-H, asym., and sym.), 1681(C=N str.), 1510(C=C ring str.), 1362(C–N str).

2.1.2 Synthesis of the Azo-Imine Ligands (L_1 and L_2) [25]

Azo-imine (azo-acen) ligands were synthesized by first preparing the ACEN diazonium salt, which was then coupled with the coupling component 4,5-diphenylimidazole (4,5DPI) to yield ligand L_1, and with 2-naphthol to produce ligand L_2, as outlined: a (5 mmole, 1.47gm) of amino group of Imine ACEN was solvated by 20% HCl solution, in an ice cold bathroom (0-5º) , then a (10mmole, 0.69gm) $NaNO_2$ dissolved by 15 ml cold D.W, was decanted dropwise to the acidic ACEN solution at the same temperature for 10 min. Then the whole solution still away for 15 min. to complete the diazonium salt formation, while the coupling component of the (L_1 10mmole 4,5-diphenyl imidazole, 2.2gm & L_2 10 mmole 2-Naphthol, 1.44gm) were dissolved individually in a 10% basic ethanolic solution and put them in the temperature, coupling process was started by the addition of the diazonium salt solution dropwise with stirring at 5º C to the solution of the coupling component, the color change was observed due azo formation, the stirring continued for 30min. and the solution was neutralized, for complete the whole solution diazotization, an azo-Imine colored precipitant developed, which was then filtered and washed twice with deionized D.W and dried.

L_1 was a light brown solid with a chemical formula ($C_{48}H_{40}N_{10}$) M.Wt 756.92 g/mole , Anal.Calc. C 76.17, N 18.51, H 5.33 found C 76.67, N 18.81, H 5.30 yield 78%, M.P. 216-218, FTIR data (cm^{-1}): 3195 (imidazole N-H str.), 3089 (Ar-H), 2979, 2844(C-H alkyl, sym. & assym.), 1597 (C=N azomethine str.), 1575(C=N imidazole str.), 1508(C=C ring

str.),1481(N=N str.), 1391(C–N str.), shown in Figure 2 ^{1}H-NMR (500 MHz, DMSO- d_6): δ 13.26 (s, 2 H, imd NH), 8.17 -7.36 (m,14H, Ar-H), 5.39 (s, 4 H, -CH_2-CH_2-C-) , 2.65 (s, 6 H, -C-CH_3), shown in Figure , ^{13}C-NMR (125 MHz, DMSO-d_6): δ 164.00 (2C of azomethine), 160.36 (2C, C_2 of imd.), 158.40 (4C, of 4,5-imd.carbons), 147.34 (2C, imd-N=N-C- of Ar ring), 142.47 (2C, -N=N-C of Aromatic ring),133-116(28C, Ar-C's) , 64.00(2 C, CH_2-CH_2), 22.41(2C - CH_3).

Mass data Z/e, M 756, M+1 757 ,220 DPI.

H_2L_2 was an Orange-reddish solid with a chemical formula ($C_{38}H_{32}N_6O_2$) M.Wt 604.71 g/mole, Anal. Calc. C 75.48, N 13.90, H 5.33, O 5.29 found C 75.88, N 14.01, H 5.35 O 5.33 yield 88%, M.P. 210-212, FTIR data (cm^{-1}): 3328 (naphthol O-H str.), 3055 (Ar-H), 3035, 2998 (C-H alkyl, sym. & asym.), 1620 (C=N azomethine str.), 1549(C=C ring str.),1490 (N=N str.), 1357(C–N str.), shown in Figure 3, ^{1}H-NMR (500 MHz, DMSO- d_6): δ 9.70 (s, 2 H, Naphthol O-H), 8.45 -7.40 (m,20 H, Ar-H), 5.74 (s, 4 H, -CH_2-CH_2-C-) , 2.57 (s, 6 H, -C-CH_3), shown in Figure, ^{13}C-NMR (125 MHz, DMSO- d_6): δ 166.00 (2C of azomethine -C=N-), 133.96 (4C, -N=N-C- Ar), 132.99 (2C, OH-C- of Aromatic ring),130.01-117.56(24C, Ar-C's) , 65.12(2 C, CH_2-CH_2), 26.64(2C - CH_3) , Mass data Z/e , M , M+1. 605,606.

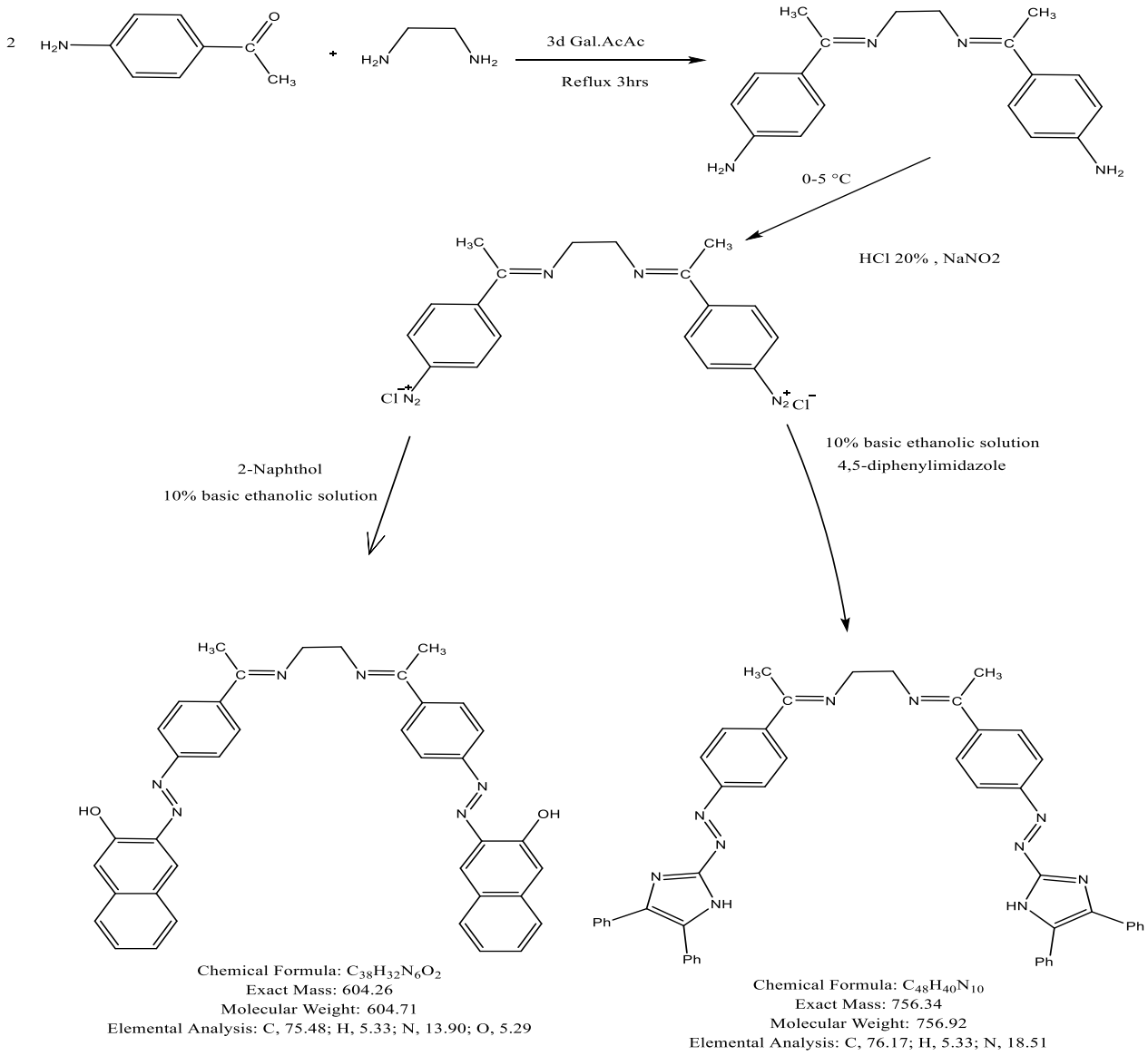

Scheme 1: Route of ligand preparation

2.1.3 Synthesis of Complexes

1. PtL_1 synthesis - The platinum complexes were prepared by dissolving 0.5 mmol (0.378 g) of the ligand L_1 in 40 ml DMSO, while 1 mmol (0.415 g) of K2PtCl4 was dissolved in 10 mL of DMSO. The K2PtCl4 solution was then added dropwise to the ligand solution. The resulting mixture was refluxed for 8 hrs. The addition of diethyl ether to the mixture at room temperature enhanced the development of the brown-orange precipitant, which was then filtered and wished several times with ether and dried in a vacuum open [26].

1. PtL_1 was an orange - brownish solid with a chemical formula ($Pt_2C_{48}H_{40}N_{10}Cl_4$), M. Wt 1288.89 g/mole, Anal. Calc. C 44.73, N 10.78, H 3.13, Cl 11.00 and Pt 30.27 found C 44.96, N 11.04, H 3.15, Cl 11.44and Pt 31.12 yield 71%, M.P. 288-290, FTIR data (cm^{-1}): 3195 (imidazole N-H str.), 3089 (Ar-H), 2979, 2844(C-H alkyl, sym. & assym.), 1615 (C=N shown in Figure 4 ^{1}H-NMR (500 MHz, DMSO- d_6): δ 12.89 (s, 2 H, imd. NH), 8.16 -7.36 (m,14H, Ar-H), 5.35 (s, 4 H, -CH_2-CH_2-C-), 2.65 (s, 6 H, -C-CH_3), Mass data Z/e, M 1286, M+1 1287.

2. PdL_2 synthesis: palladium complex was synthesized via the dropwise addition of (1 mmole, 0.259 gm) bis acetonitrile palladium dichloride in 20 ml methanol to the ligand suspension solution (0.5mmole, 0.303 gm) in 40 ml methanol, then refluxed for 6hrs. After cooling, the complexes precipitant was developed and separated by filtration followed by washing with 30 ml methanol and drying by oven [27].

PdL_2 was an orange-reddish solid with a chemical formula ($Pd_2C_{38}H_{34}N_6O_4Cl_2$) M.Wt / 922.47 g/mole , Anal.Calc. C 49.48, N 9.11, H 3.72, Cl 7.69 and Pd 23.07 found C 49.96, N 9.34, H 3.75, Cl 7.94and Pd 24.09 yield 77%, M.P. 265-268, FTIR data (cm^{-1}): 3053 (Ar-H), 3035, 2998(C-H alkyl, sym. & assym.), 1620 (C=N azomethine str.), 1551(C=C ring str.),1483 (N=N str.), 1402(C–N str.), shown in Figure 5 ^{1}H-NMR (500 MHz, DMSO- d_6): δ 8.45 -7.40 (m,20H, Ar-H), 5.72 (s, 4 H, -CH_2-CH_2-C-) , 2.57 (s, 6 H, -C-CH_3). Mass data Z/e, M 922, M+1 923,604.

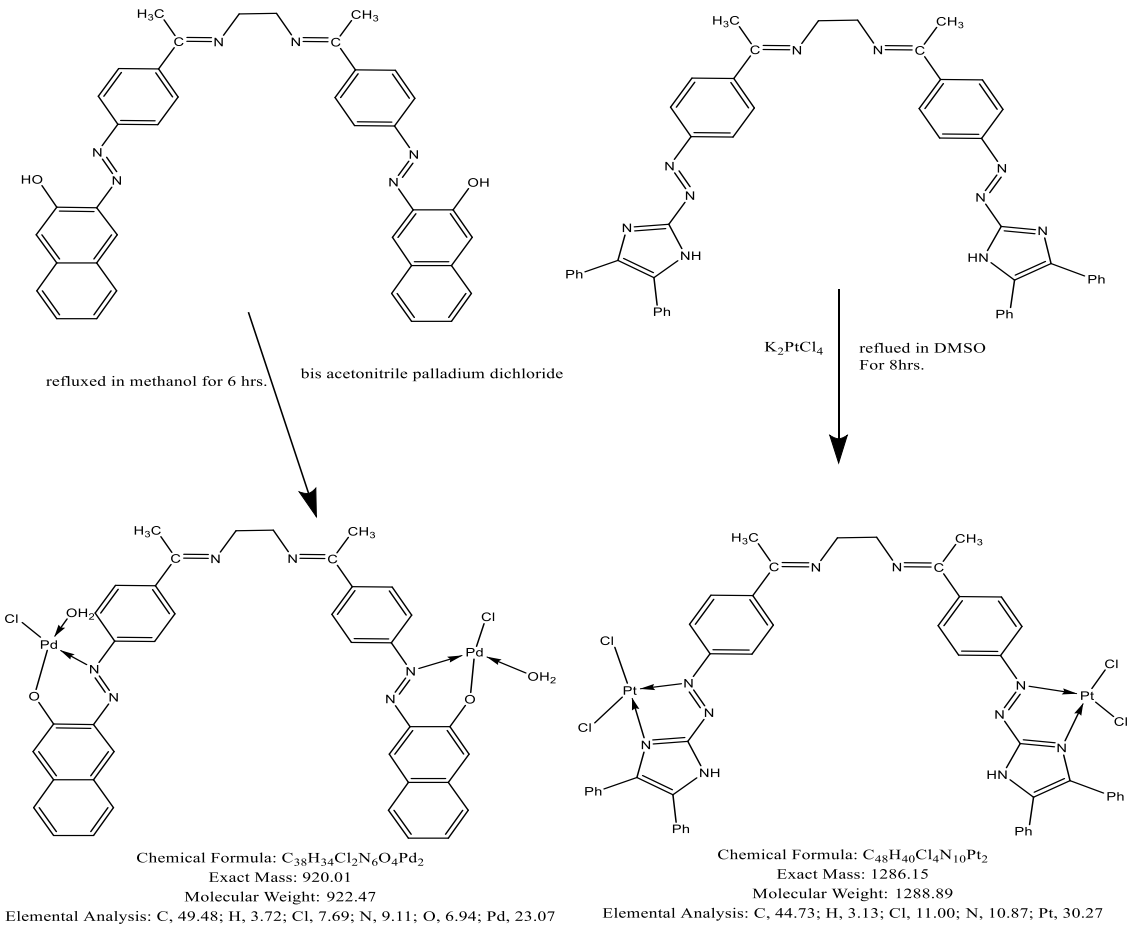

Scheme 2: Route of complex preparation

2.2 Antibacterial Test for Metal Complexes

The activity of the metal complexes was evaluated using the Minimum Inhibitory Concentration (MIC) and Minimum Bactericidal Concentration (MBC) methods, as described by Mahdieh et.al. [28] following the approved guideline M26-A. The concentration limit of the study (9.7-5000) µg/ml.

2.3 DPPH Radical-Scavenging Assay

A Modified Brand–William's method presented by Miliauskas et.al. [29] was used in determining the antioxidants capacity using the DPPH radical-scavenging capacity of the prepared samples. Briefly, DPPH• solution (200 millimolar, in ethanol) was mixed with the samples. The reaction mixture sample was incubated for 1 hr. at 25 °C in the dark. The reaction of the DPPH radical was estimated by measuring the absorption at 517 nm against ethanol as a blank in the spectrophotometer. The percentage of the DPPH• scavenging inhibition capacity was calculated from Equation:

$$\%\, Inhibition = [1 - (Absorbance\ of\ sample / Absorbance\ of\ control)] \times 100$$

The concentration limit of the samples was (1.5 – 32 µg/ml).

2.4 MTT Protocol

MCF-7 human breast cancer cell line was supplied from the American Type Culture Collection (ATCC, Manassas, VA, USA). The protocol was applied as described by Dhekra and Saad [30] and the results were given as the mean of three independent experiments with (1000, 500, 250, 125, 62.5, 31.25, and 0 µg/ml concentration limits. Concentrations of samples showing a 50% reduction in cell viability (i.e., IC_{50} values) were then calculated.

3. Results and Discussion

3.1 Synthesis

Both ligands and their complexes were solid powders, hygroscopic, and non-soluble in water, but they're soluble in most organic solvents such as acetone, chloroform, dichloromethane, DMF, DMSO, ethanol, methanol. They were analyzed using UV-visible, FTIR, NMR, Mass, magnetic susceptibility, and molar conductance; the analytical results align well with the calculated values, as the anticipated formula $[M_2L_1Cl_4]$ corresponds to M = Pt (II) and $[M_2L_2(H_2O)_2Cl_2]$ for M = Pd (II), both exhibiting a [M: L] 2:1 stoichiometry, the analytical data, along with the physical properties, are presented in Table 1.

Table 1: Physical properties of the synthesized compounds

Compound	FW gm/mole	m.p	yield	Elementary analysis Found (cal.) %				$\Lambda_M\ \Omega^{-1}\ Cm^{-1}\ mol^1$	λ_{max}
				C	H	N	M		
$C_{48}H_{40}N_{10}$ L_1	756.92	112-114	82%	76.67 (76.17)	5.30 (5.33)	18.81 (18.51)	———	-------	398 nm
$Pt_2C_{48}H_{40}N_{10}Cl_4$ PtL_1	1288.89	231-233	77%	44.96 (44.73)	3.15 (3.13)	11.04 (10.78)	31.12 (30.27)	18	462 nm
$C_{38}H_{32}N_6O_2$ L_2	604.71	176-178	88%	75.88 (75.48)	5.35 (5.33)	14.01 (13.90)	------	-------	378 nm
$Pd_2C_{38}H_{34}N_6O_4Cl_2$ PdL_2	922.47	257-259	72%	49.96 (49.48)	3.75 (3.72)	9.34 (9.11)	24.09 (23.07)	22	413 nm

3.2 FTIR Spectral Study

The FTIR spectra provide important and valuable information about the presence and nature of the organic compound's functional groups and their coordination in complexes [31], an IR spectral comparison between the ligands and their complexes regards one of the types of evidence for functional groups binding in coordination to the metal ions in their complexes.

Beginning from the Imine base (ACEN), its IR spectra clearly showed its mean functional group as the primary amine ($-NH_2$ at 3248&3166 cm^{-1} str.), and the azomethine (-C=N -) at 1681 cm^{-1} as shown in Figure 1.

Table 2: Mean FTIR Frequencies (cm^{-1}) of the Prepared Compounds

no.	compound	-OH Coor.H_2O	imd-NH NH_2	-C=N- Im-C=N-	-N=N-	M-O M-N	M-Cl
1	ACEN ($C_{18}H_{22}N_4$)	---------	3248str. 3166str.	1681	----------	-------	-------
2	L_1 ($C_{48}H_{40}N_{10}$)	---------	3195	Im. 1597 Imd. 1575	1481	----------	----------
3	$Pt_2(C_{48}H_{40}N_{10}Cl_4)$	--------	3195	Im 1597 Imd 1570	1451	482	431
4	H_2L_2 ($C_{38}H_{32}N_6O_2$)	3328	----------	1620	1490	----------	----------
5	$Pd_2(C_{38}H_{34}N_6O_4Cl_2)$	3480 Coor.H_2O	----------	1620	1483	694	-----

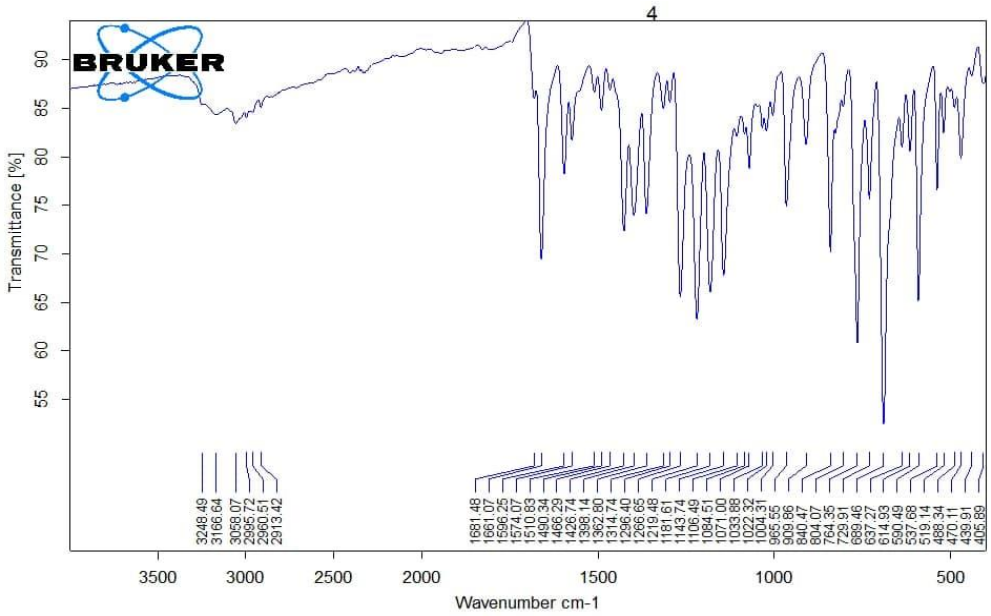

Figure 1: FTIR spectra of acen Imine

The L_1 ligand spectra show a clear N-H imidazole band at 3195 cm^{-1} with the disappearance of the primary amine band due to diazoation, the imidazole ring (-C=N-) was observed at 1557 cm^{-1} and an azo bridge group (-N=N-) at 1481 cm^{-1} , while its platinum complexes PtL_1 show an alteration in the imidazole ring (-C=N-) group and azo group (-N=N-) shown at 1570 & 1451 cm^{-1} respectively due to the participation of the N atoms lone pairs of these groups in the coordination with vacant orbitals of the central platinum ion and complex formation, the Pt-N and Pt-Cl absorption bands were present at 482 & 431 cm^{-1}, While other groups do not participate in the coordination, this is evident in Figs. 2a and 2b.

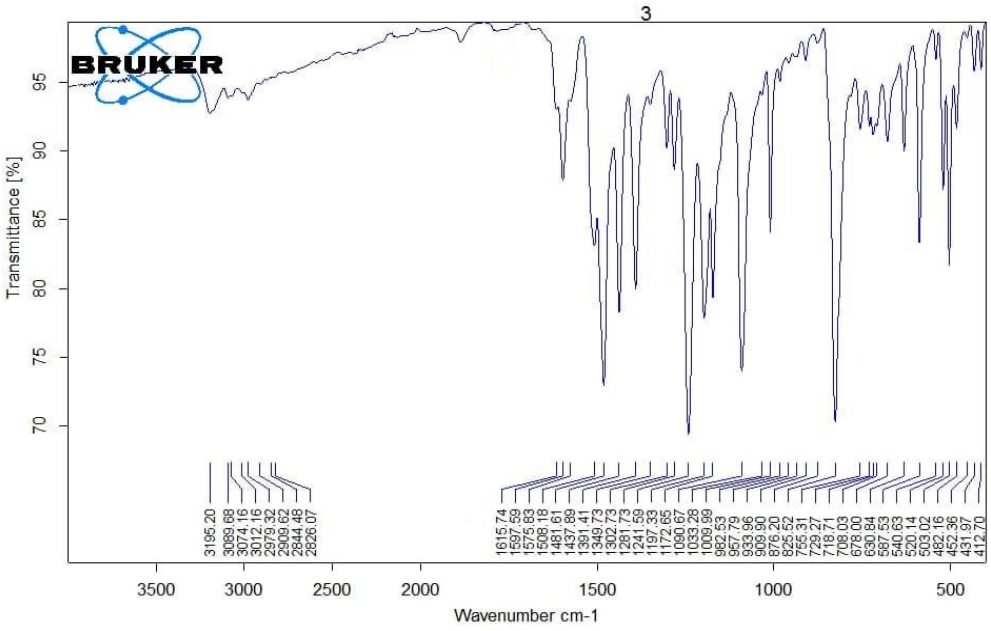

Figure 2:a FTIR spectra of L_1

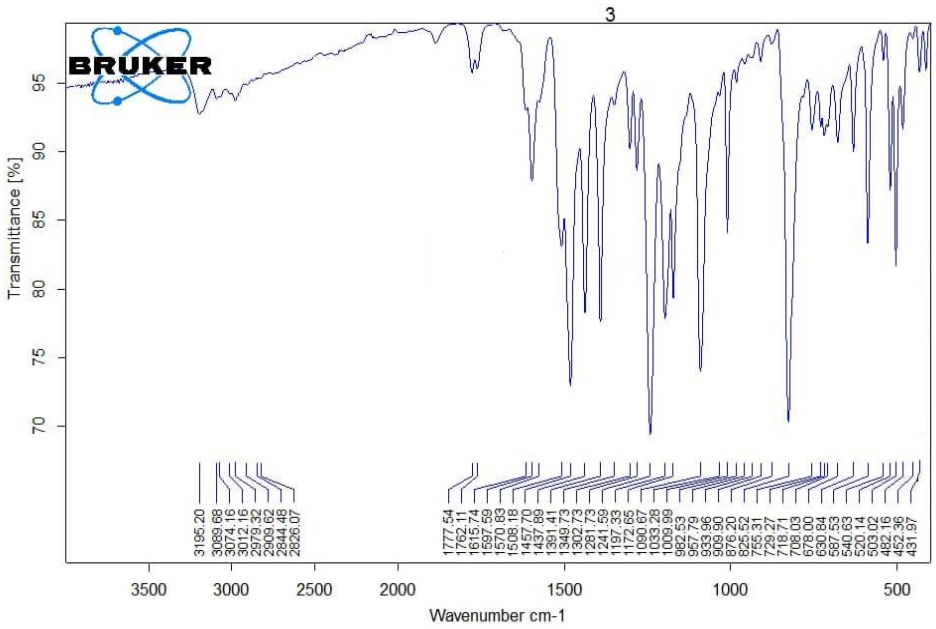

Figure 2: b FTIR spectra of PtL_1

The FTIR spectra of the second ligand L_2 enhanced for the determination of many important functional groups as the naphtholic hydroxyl group at 3328 cm^{-1} , an azomethine group at 1620 cm^{-1} and the N=N azo group at 1490 cm^{-1} , the less important group were found in the same spectra such the aryl and alkyl C-H bands at 3055 (Ar-H), 3035, 2998 (C-H alkyl, sym. & asym.), 1620 and the aromatic (C=C ring 1549 str.), while the palladium complex PdL_2 spectra show the disappearance of the hydroxyl group band due the deprotonation and the covalent – coordination banding of the oxygen atom to the palladium ion orbitals [11] and the coordinated water [32] appeared at 4480 cm^{-1}. The azo group participates in coordination through its nitrogen atom's lone pair, as indicated by the lowering in its stretching band and appeared at 1484 cm^{-1}. This results in the formation of a bidentate chelating complex with the palladium ion, taking into account that the azomethine group doesn't participate in the coordination. The ligand and its complex are illustrated in Figures 3a and 3b.

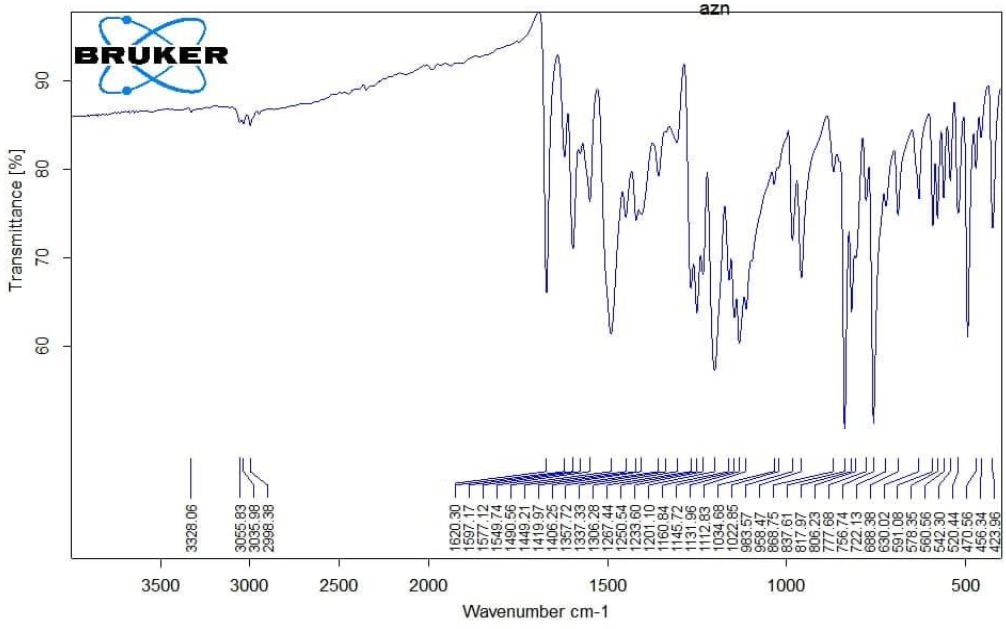

Figure 3:a FTIR spectra of L_2

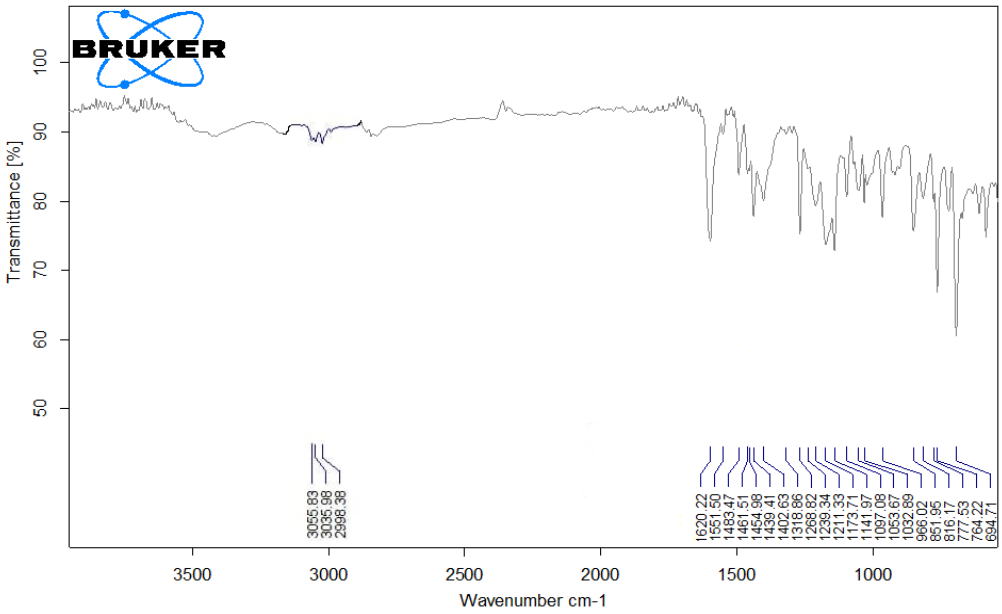

Figure 3: b FTIR spectra of PdL_2.

3.3 Mass Spectral Study

A mass spectra technique is a crucial analytical tool used to elucidate the structure of numerous organic and inorganic compounds by determining their masses, and molecular structures and suggesting their fragmentation routes [33] that serve to mechanism's study meanwhile.

The mass data of the azo- imine ligands and their Transition metal complexes were obtained at 298 K , using them for comparison with the suggested stoichiometric compositions, that L_1 shows a molecular peak at 756 m/z compatible with the ligand mass and a 220 m/z that equal to the diphenyl imidazole fragment, while PtL_1 complex shows the mother ion peak at 1286 m/z that equivalence to its mass, and the ligand fragment was also observed at 756 m/z.

L_2 spectra and its Palladium complex were recorded at a mother peak at 605 and 920 m/z respectively, that agreed with their masses, the mass data are shown in Figures 4a, b and 5a, b.

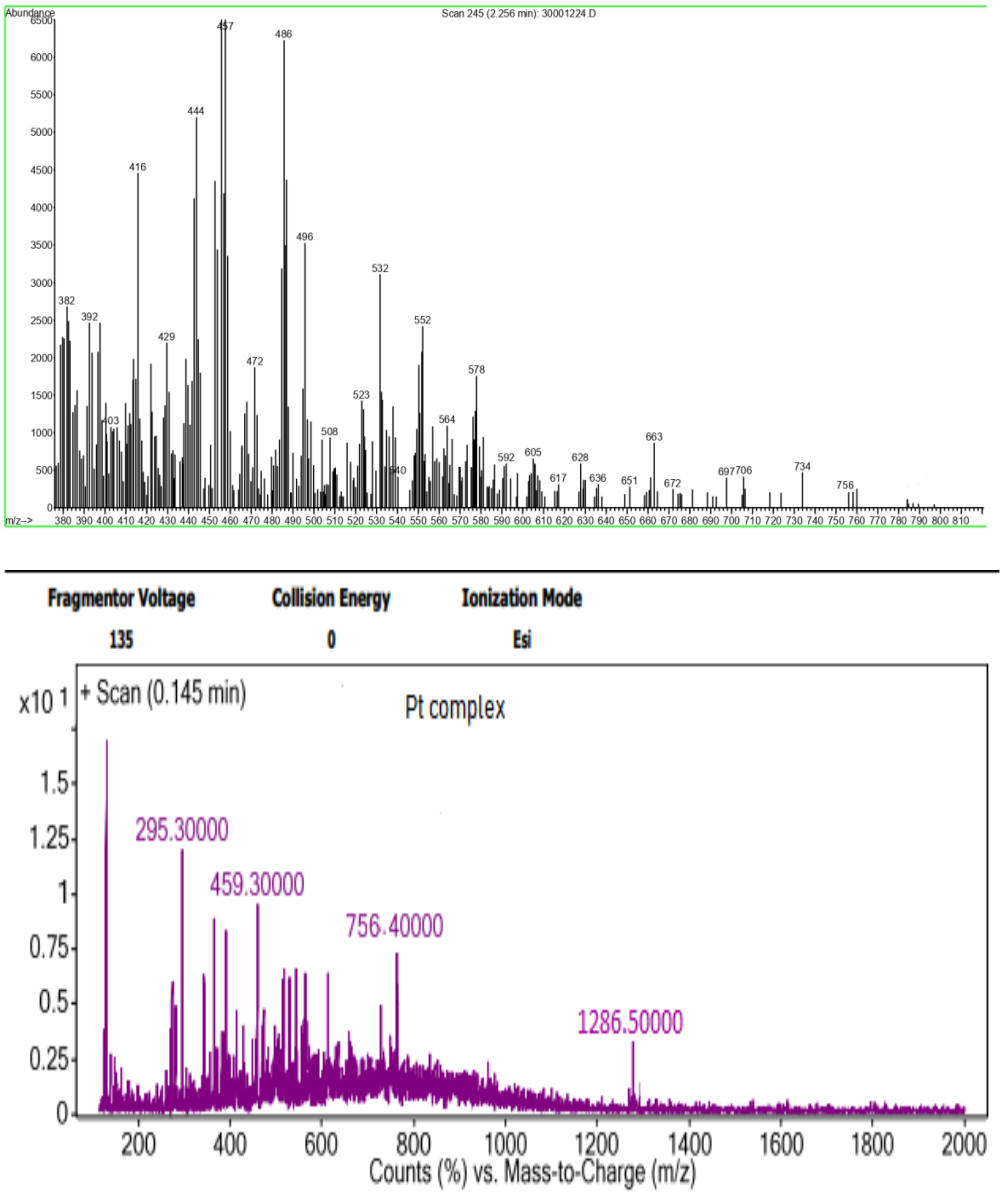

Figure 4:a, b The mass spectra of the L_1 and complex PtL_1.

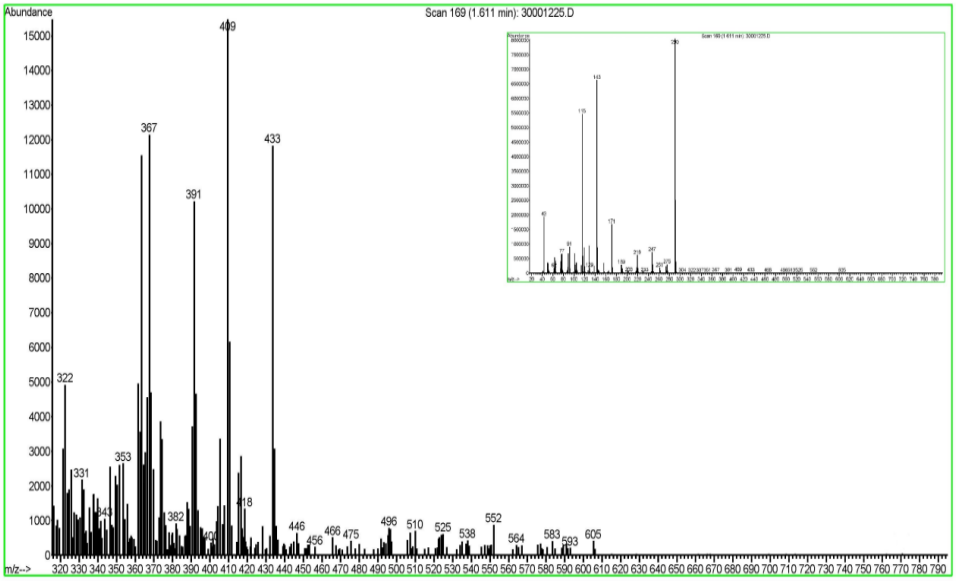

Figure 5:a Mass spectra of the L_2 Ligand

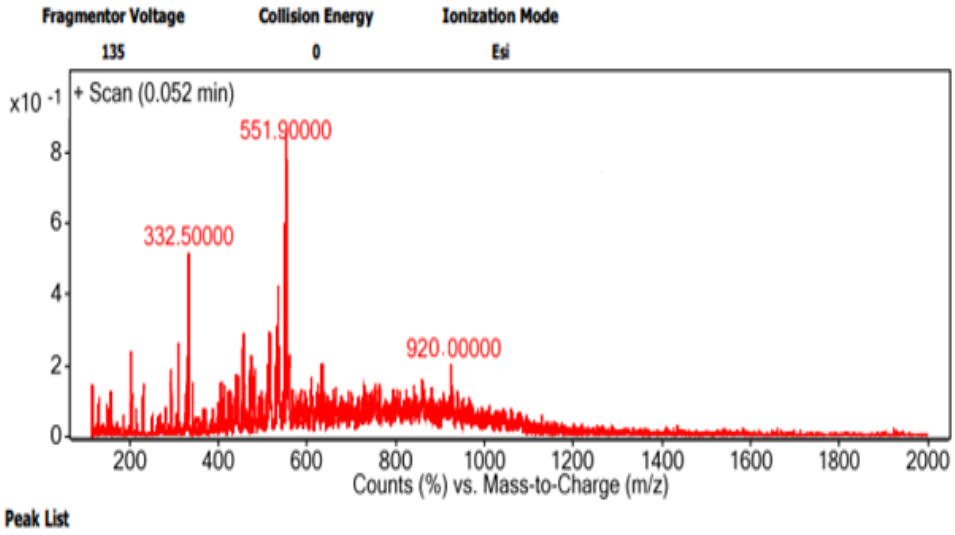

Figure 5: b Mass spectra of the PdL_2 Complex

3.4 NMR Spectroscopy

An important technique used for the determination of the organic molecules in solution is when the FTIR illustrated the present functional groups. ^{1}HNMR provides valuable insight into the quantity of magnetically unique hydrogen nuclei that are being analyzed, together with the distinctive traits of the nearby environment of every unique variety [33]. From the L_1 ^{1}HNMR spectrum, an imidazole NH proton was present in δ 13.26 , the aromatic rings protons were seen at 8.17 -7.36 , while the ethylene protons 5.39 and the methyl protons of the acetophenone methyl group observed at 2.65 ppm, while its platinum complexes reveal the imidazole ring system was influenced as a result of coordination and hence the NH proton up fielded to 12.98ppm , while the aromatic ring protons were slightly affected by the complex formation as shown in Figures 6a and 6b.

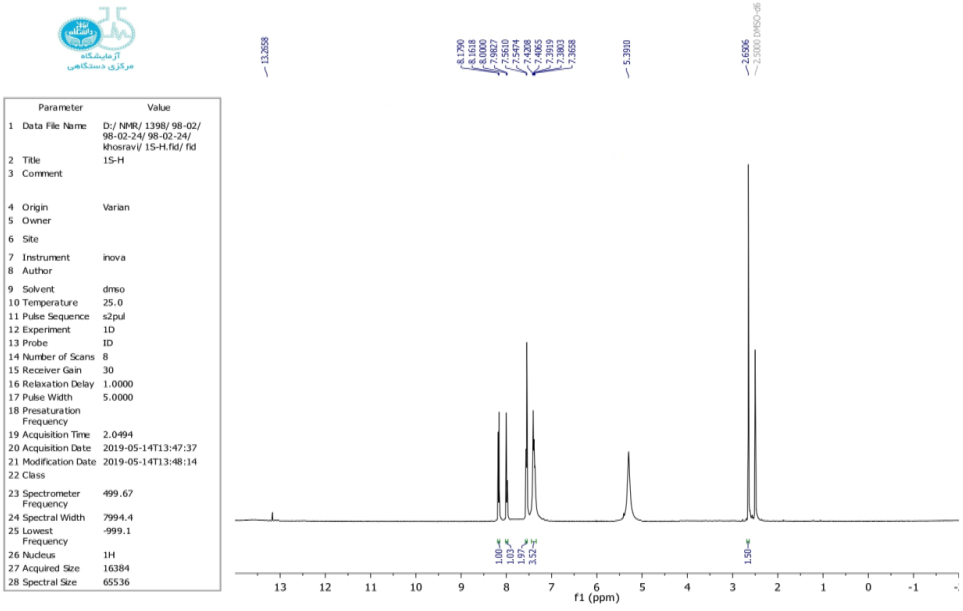

Figure 6:a The ^{1}HNMR of the L_1 complex

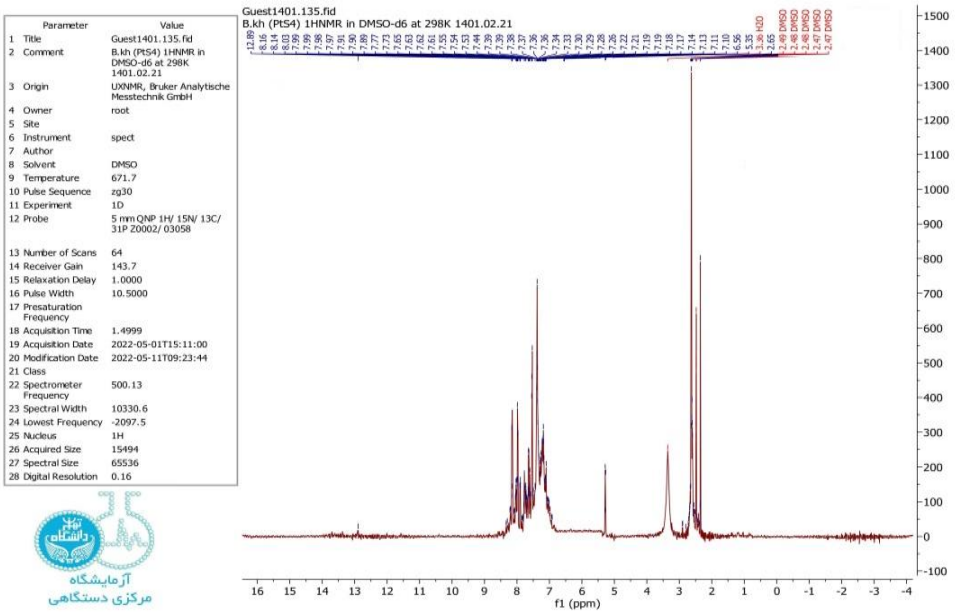

Parameter	Value
1 Title	Guest1401.135.fid
2 Comment	B.kh (Pt54) 1HNMR in DMSO-d6 at 298K 1401.02.21
3 Origin	UXNMR, Bruker Analytische Messtechnik GmbH
4 Owner	root
5 Site	
6 Instrument	spect
7 Author	
8 Solvent	DMSO
9 Temperature	671.7
10 Pulse Sequence	zg30
11 Experiment	1D
12 Probe	5 mm QNP 1H/ 15N/ 13C/ 31P Z0002/ 03058
13 Number of Scans	64
14 Receiver Gain	143.7
15 Relaxation Delay	1.0000
16 Pulse Width	10.5000
17 Presaturation Frequency	
18 Acquisition Time	1.4999
19 Acquisition Date	2022-05-01T15:11:00
20 Modification Date	2022-05-11T09:23:44
21 Class	
22 Spectrometer Frequency	500.13
23 Spectral Width	10330.6
24 Lowest Frequency	-2097.5
25 Nucleus	1H
26 Acquired Size	15494
27 Spectral Size	65536
28 Digital Resolution	0.16

Figure 6: b The ^{1}HNMR of the PtL_1 complex

The other ligand L_2 ^{1}HNMR spectra show a clear singlet signal at δ 9.70 ppm related to the naphtholic hydroxyl proton [34], multiple aromatic signals in the range (8.45-7.40) and an aliphatic protons signal at 5.47 & 2.57 ppm related to the ethylene and methyl groups respectively, meanwhile, its palladium complex spectra show the disappearance of the hydroxyl proton signal due the deprotonation and oxygen atom coordination to the palladium ion vacant orbital and complex. The formation of the complex had a slight effect on the aromatic ring protons, while the aliphatic protons remained unaffected by coordination. The NMR spectra of the ligand and its complex are presented in Figures 7a and 7b.

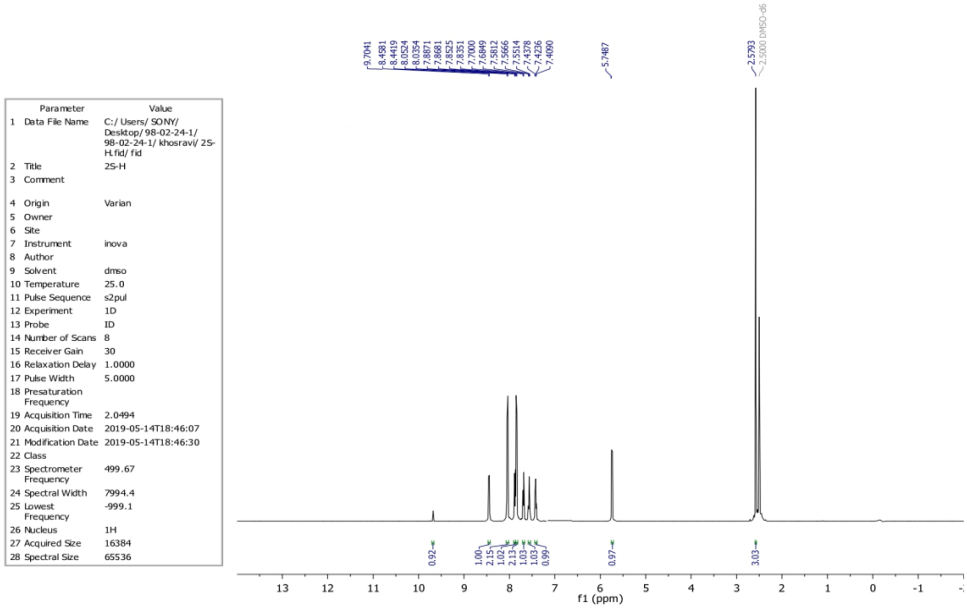

Parameter	Value
1 Data File Name	C:/ Users/ SONY/ Desktop/ 98-02-24-1/ 98-02-24-1/ khosravi/ 25-H.fid/ fid
2 Title	25-H
3 Comment	
4 Origin	Varian
5 Owner	
6 Site	
7 Instrument	inova
8 Author	
9 Solvent	dmso
10 Temperature	25.0
11 Pulse Sequence	s2pul
12 Experiment	1D
13 Probe	ID
14 Number of Scans	8
15 Receiver Gain	30
16 Relaxation Delay	1.0000
17 Pulse Width	5.0000
18 Presaturation Frequency	
19 Acquisition Time	2.0494
20 Acquisition Date	2019-05-14T18:46:07
21 Modification Date	2019-05-14T18:46:30
22 Class	
23 Spectrometer Frequency	499.67
24 Spectral Width	7994.4
25 Lowest Frequency	-999.1
26 Nucleus	1H
27 Acquired Size	16384
28 Spectral Size	65536

Figure 7: a The ^{1}HNMR of the L_2

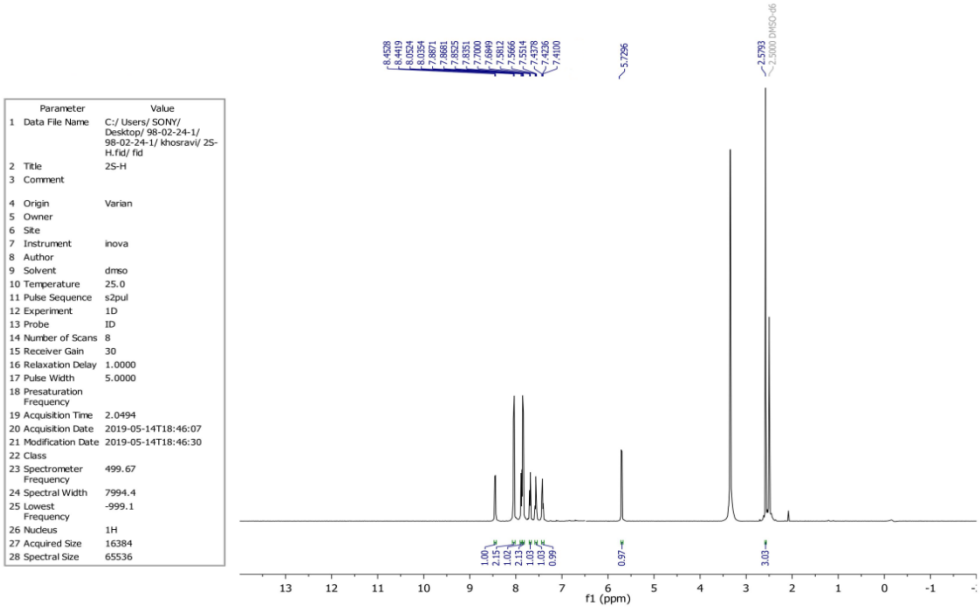

Figure 7: b The ^{1}HNMR of the PdL_2 complex

^{13}CNMR Spectroscopy is an important technique widely used for characterizing organic and organometallic compounds [35]. It offers simplicity and high sensitivity to structural differences. The ^{13}CNMR spectra of the L_1 ligand reveal some important carbon environments such δ 164.00 (2C of azomethine), 160.36 (2C, C_2 of imd.), 158.40 (4C, of 4,5-imd.carbons), 64.00(2 C, CH_2-CH_2) and the methylene one 22.41(2C - CH_3) that clearly shown in Figure 8a, while the other ligand L_2 spectra give an important carbon environments as observed in Figure 8b such: the δ 166.00 (2C of azomethine -C=N-), 133.96 (4C, -N=N-C-Ar), 132.99 (2C, OH-C- of Aromatic ring) , 65.12(2 C, CH_2-CH_2), 26.64(2C - CH_3).

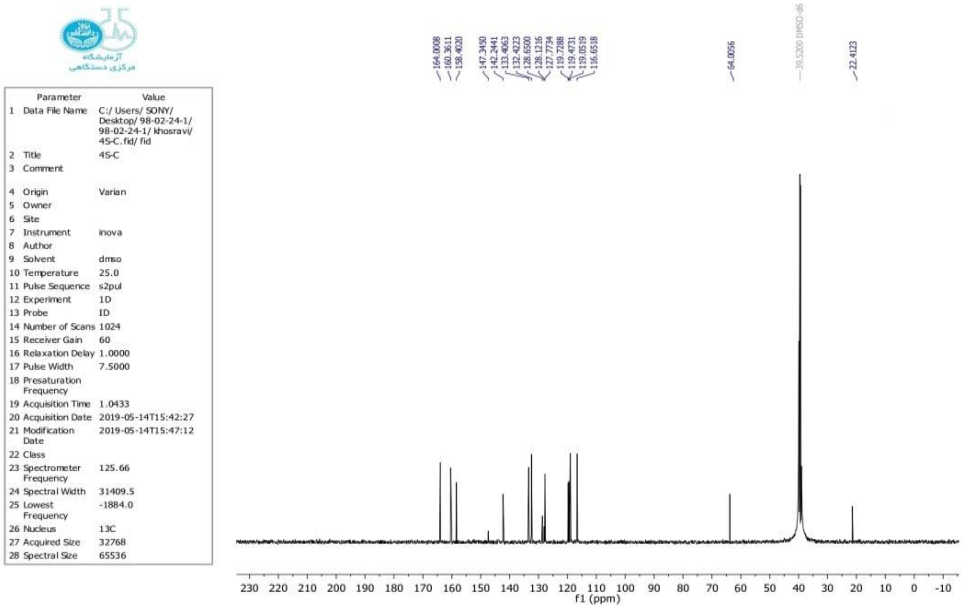

Figure 8: a ^{13}CNMR of the L_1 ligand

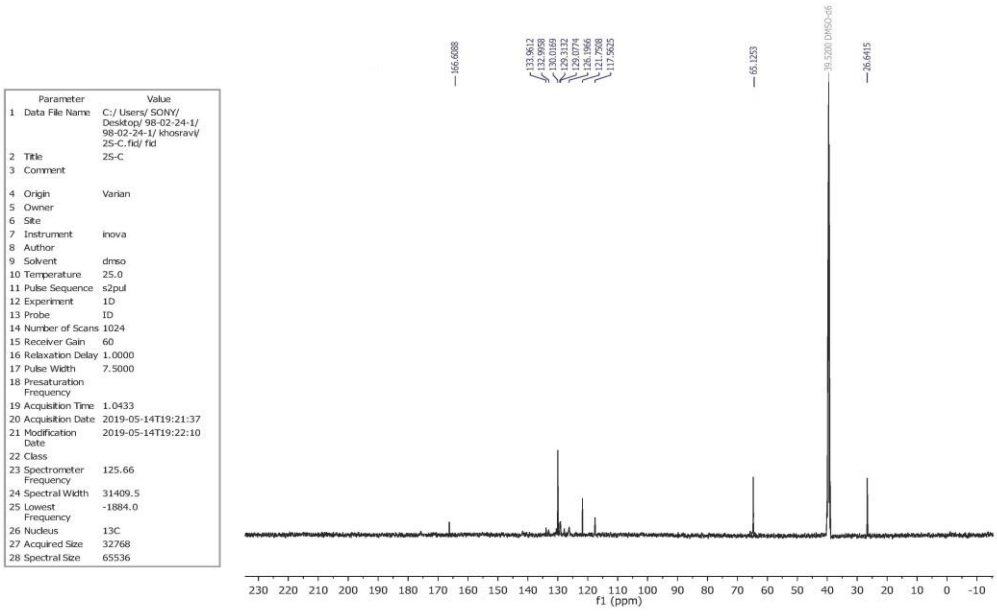

Figure 8: a ^{13}CNMR of the L_2 ligand

3.4 UV-Vis Spectroscopic Study

The Ultraviolet –Visible spectrum of the synthesized ligands and their complexes were recorded in ethanol solvent (5 X 104- M) within the working instrument range (200-700) nm , the azo group present in the molecule led to the(π-π*) [33] transition appears at 398 and 378 nm for L_1 &H_2 L_2 respectively, as shown in their spectra's, while their mixing solutions with the selected ions exhibit a bathochromic shifting toward (red shifting) toward higher wavenumber that the first ligand (PdL_1 and PtL_1) complexes absorbed at (470 and 462nm) , while the second ligand (PdL_2 and PtL_2) complexes give an absorbance maxima at (418 and 443 nm) respectively. This phenomenon occurs due to the participation of the ligand's lone pairs in the coordination with the vacant ionic orbitals. Additionally, the formation of these new complexes results in color changes in the ligands. The spectra of the ligands and their complexes are illustrated in Figures 9a and 9b.

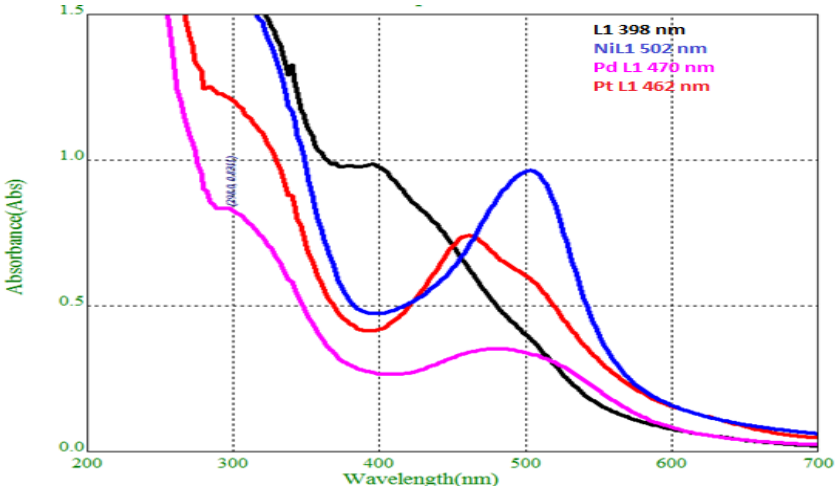

Figure 9: a The ultraviolet-visible spectrum of L_1 and its complexes.

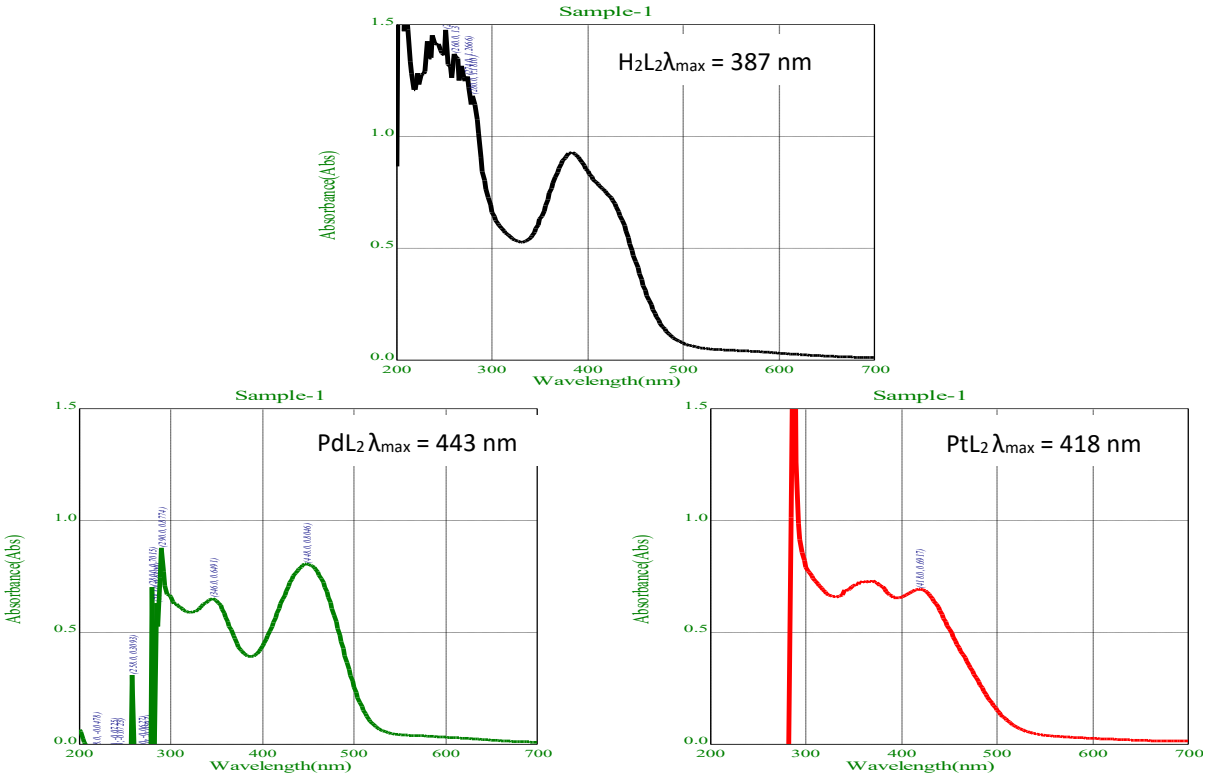

Figure 9: b The Ultraviolet-Visible spectrum of L_2 and its complexes.

3.5 Molar Conductance and Magnetic Susceptibility

The molar conductance of the PtL_1 and PdL_2 complexes at 10-3M, using DMSO solvent and room temperature were (18 and 22) Ω-1cm^2 mol^{-1}, these low values indicate the non-electrolyte of these complexes and there were no counter chloride or water molecules and hence it can suggest that the water molecule complete the coordination sphere of PdL_2 complex [36].

The magnetic susceptibility of these complexes approaches zero, as shown in the table, which suggests that they exhibit diamagnetic behavior, characteristic of square planer d^8 complexes.

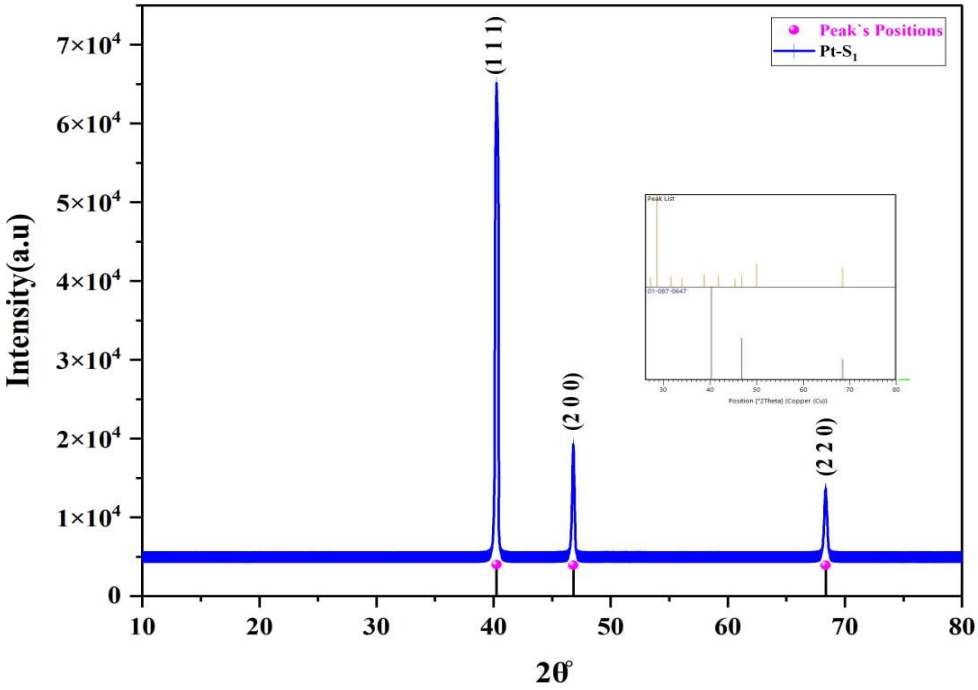

Figure 10: a XRD Spectra of PtL_1

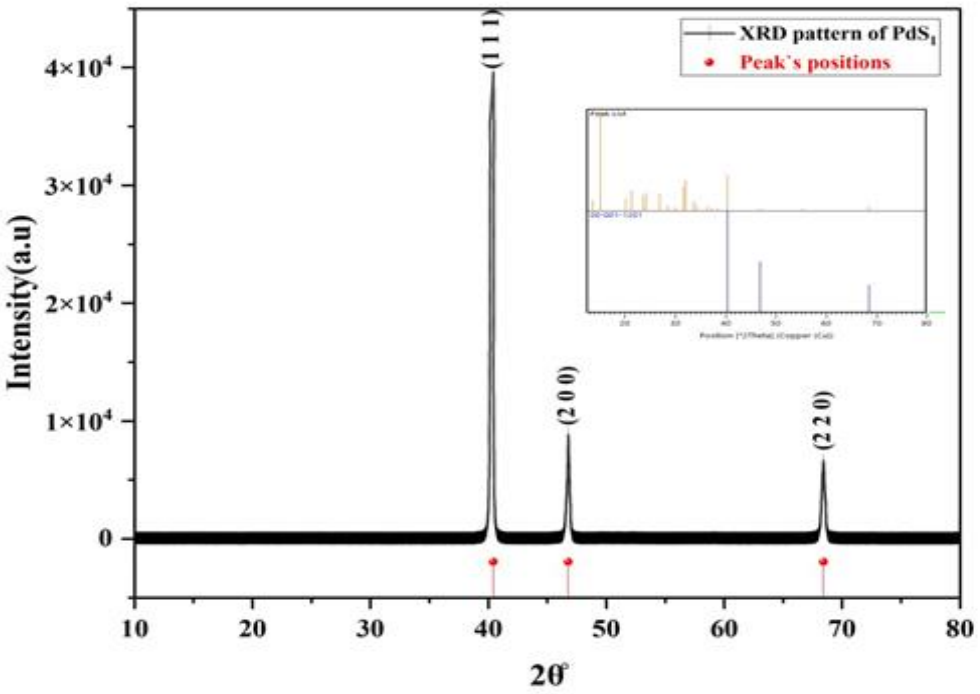

Figure 10: b XRD Spectra of PdL_2

Table 3: Grain size calculation from XRD data for PdL_2 and PtL_1 complexes.

PtL_1 Complex			
Peaks Positions (2θ°)	**FWHM(β)**	**Grain Size(nm)**	**Average grain Size(nm)**
40.26275	0.25207	33.55387034	34.03456318
46.80132	0.23499	36.82239769	
68.35321	0.30254	31.72742151	
PdL_2 Complex			
Peaks Positions (2θ°)	**FWHM(β)**	**Grain Size(nm)**	**Average grain Size(nm)**
40.2936	0.24616	34.36285005	30.23414926
46.78068	0.29796	29.03819628	
68.40748	0.3517	27.30140144	

3.7 Biological Studies

Three biological parameters were evaluated for the new compounds. Specifically, the antibacterial activity of the PtL_1 and PdL_2 complexes was assessed through the determination of the minimum inhibition concentration (MIC) and minimum bacterial concentration (MBC) using two different types of gram response bacteria, as mentioned in Table 4. with their laboratory results.

Table 4: The MIC and MBC data for the study complexes.

I.	Strain: *Staphylococcus aureus ATCC 25923*	Gram-Positive Bacteria
Sample	**PtL_1**	**PdL_2**
MIC (µg/ml)	>5000	625
MBC(µg/ml)	>5000	2500
II	Strain: *Escherichia coli ATCC 25922*	Gram Negative Bacteria
Sample	**PtL_1**	**PdL_2**
MIC (µg/ml)	>5000	5000
MBC(µg/ml)	>5000	

The tested complexes were reported to have a greater antibacterial effect on the gram-positive index of *Staphylococcus aureus* than the gram-negative index of *Escherichia coli*.

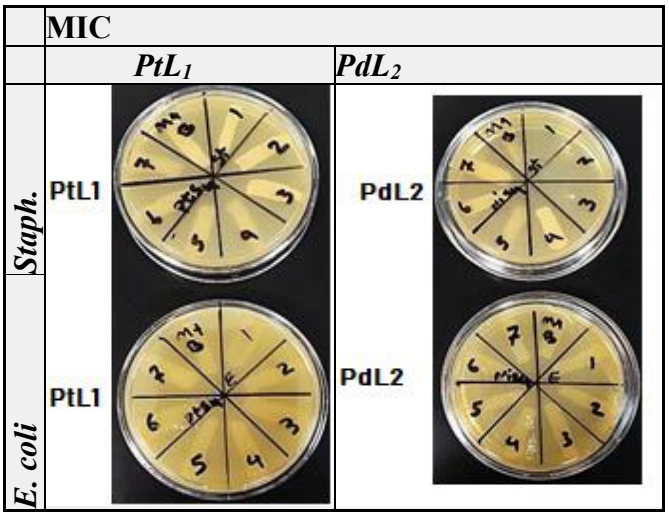

Figure 11: a MIC for the selected complexes

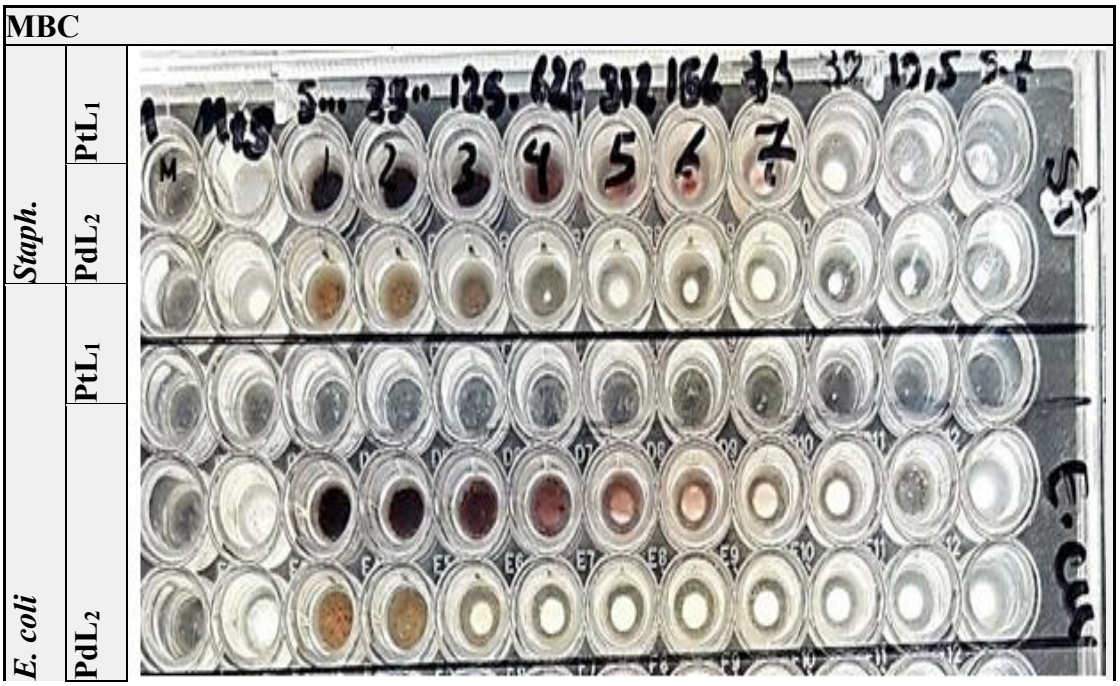

Figure 11:b The MBC of the PtL_1 and PdL_2

In this method, the PdL_2 complex demonstrated a stronger antibacterial effect compared to PtL_1, particularly when considering sufficient bacterial activity for the same species for the palladium and platinum complexes were utilized [39].

1. **Antioxidant study**

The antioxidant capacity of the newly synthesized compounds was measured using the DPPH assay, which assesses their radical scavenging ability [40]. The newly synthesized compounds were tested for antioxidant scavenging and the results are shown in Figure 12, the work was conducted with three replicas and the average of them was adopted for calculation using DPPH as a control.

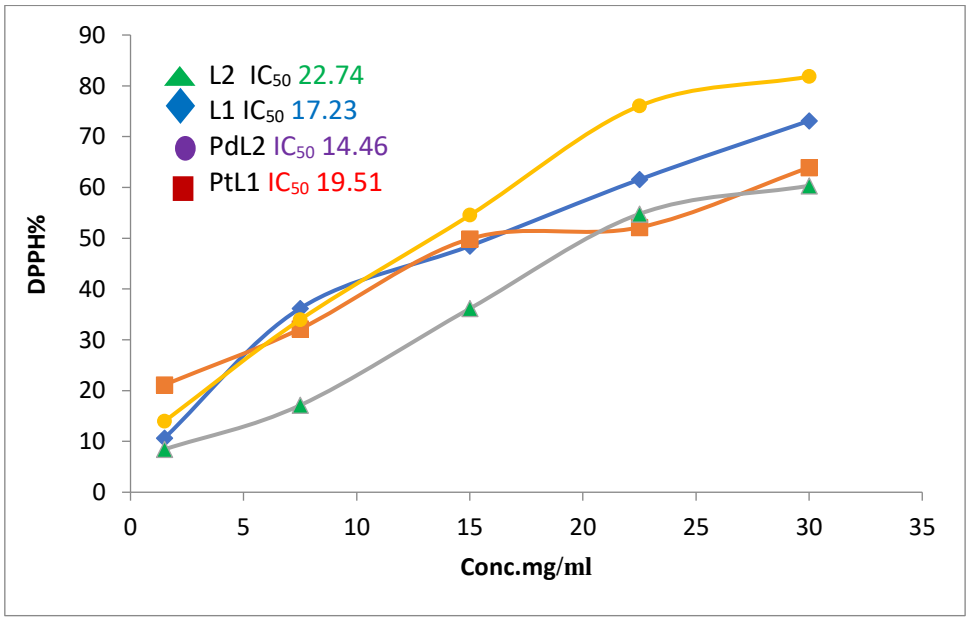

Figure 12: DPPH scavenging capacity and the IC_{50} values in mg/ml for the new compounds.

The antioxidant data depicted that the PdL_2 complex with the IC_{50} 14.46 µg/ml is more effective as an antioxidant than its ligand and the other studied compounds.

3.8 MCF7 Cell Line Study

An MTT method for breast cancer MCF7 cell line was examined for the comparison between PtL_1 and PdL_2 in their effectiveness on breast cancer cells, the results observed that the platinum complex was more active than the palladium complex toward breast cancer cells as shown in Table 5 and Figures 13 & 14.

Table 5: Breast cancer MC7 cell line for PtL_1 & PdL_2 Complexes.

Concentration µg/mL	Log Conc. µg/ mL.	PtL_1 MC7 cell line IC_{50} =28.46 µg/ mL		PdL_2 MC7 cell line IC_{50} = 40.83 µg/ mL	
		Viability%	Cytotoxicity%	Viability %	Cytotoxicity%
31.25	1.49	88.68286	11.32	94.07008	5.93
62.5	1.79	83.12020	16.88	88.4097	11.59
125	2.09	71.20205	28.8	83.22102	16.78
250	2.39	66.60358	33.4	75.96496	24.04
500	2.69	56.8798	43.13	63.78706	36.21
1000	3	39.2711	60.73	40.71429	59.28

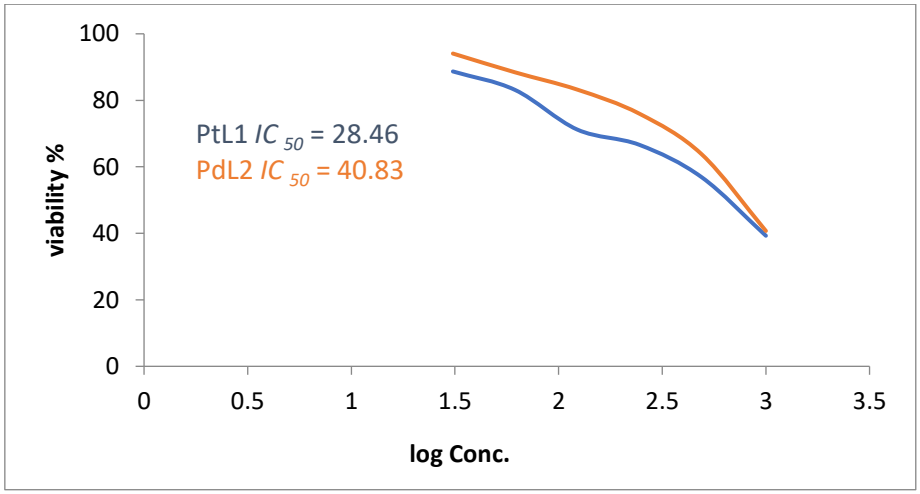

Figure 13: MCF7 Cell line for the study complexes

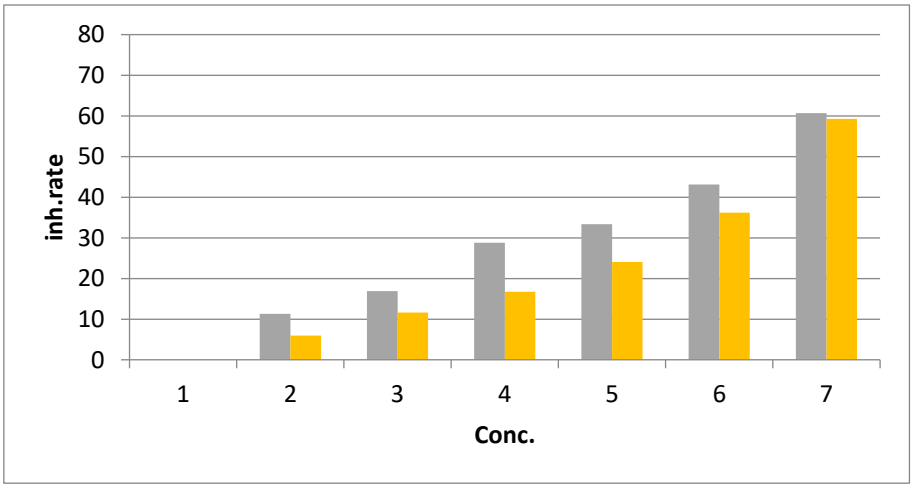

Figure 14: The inhibition rate (cytotoxicity %) of the complexes within the studied concentration.

They can show that the PtL_1 complex has an IC_{50} value 28.46 ppm which is more than the value of the palladium complex 40.83 μg/ml, this is due to the platinum ion having more charge density than the palladium ion, which made them coordinate more tightly to the breast cancer DNA nucleic acid. However, they were less than the effect of the cisplatin drug IC_{50} 4 μg /ml as a comparison for the MCF7 cell line [41].

4. Conclusions

Two novel bis azo acen (acetophenone ethylene diamine) Imine, specifically the PtL_1 and PdL_2 complexes, were synthesized and subsequently characterized utilizing a variety of spectroscopic methodologies, including FTIR, UV-Visible spectroscopy, elemental analysis, NMR, mass spectrometry, and X-ray diffraction. Additionally, supplementary methods, including conductivity evaluations and magnetic susceptibility analyses, were utilized. The spectral and analytical data substantiate PtL_1 complex coordination occurs via the imidazole ring N3 atom and the nitrogen of the azo group, while for the PdL_2 complex, coordination takes place between the azo nitrogen atom and the oxygen atom of the naphtholic ring. These ligands act as bidentate chelating agents, potentially forming diamagnetic square planar complexes. The analysis of crystalline morphology and the average particle size indicates that the synthesized complexes were prepared at the nanoscale. These complexes were subjected to biological evaluation concerning their antibacterial efficacy against the gram-negative Escherichia coli ATCC 25922 and the gram-positive Staphylococcus aureus ATCC 25923 species, yielding results that indicate the palladium complex PdL_2 exhibits greater activity than the platinum complex PtL_1. A similar observation was noted in the DPPH antioxidant assay, wherein the palladium complex PdL_2 demonstrated superior capacity compared to both the platinum complex and the associated ligands, with an IC_{50} value of 14.46 ppm. Conversely, the platinum complex PtL_1 surpassed the palladium complex PdL_2 in terms of efficacy against breast cancer cells within the MCF7 cell line, as evidenced by a minimum IC_{50} value of 28.64 μg/ml.

References

[1] M.-Y. Zhao, Y.-F. Tang, and G.-Z. Han, "Recent Advances in the Synthesis of Aromatic Azo Compounds," *Molecules,* vol. 28, no. 18, p. 6741, 2023.

[2] R. Ganjoo, C. Verma, A. Kumar, and M. A. Quraishi, "Colloidal and interface aqueous chemistry of dyes: Past, present and future scenarios in corrosion mitigation," *Advances in Colloid and Interface Science,* vol. 311, p. 102832, 2023/01/01/ 2023.

[3] S. Benkhaya, S. M'Rabet, and A. El Harfi, "Classifications, properties, recent synthesis and applications of azo dyes," *Heliyon,* vol. 6, no. 1, p. e03271, 2020.

[4] P. Barciela, A. Perez-Vazquez, and M. A. Prieto, "Azo dyes in the food industry: Features, classification, toxicity, alternatives, and regulation," *Food and Chemical Toxicology,* vol. 178, p. 113935, 2023/08/01/ 2023.

[5] R. J. Chudgar and J. Oakes, "Dyes, Azo," in *Kirk-Othmer Encyclopedia of Chemical Technology*, 5th ed. New York: John Wiley & Sons, Inc., 2000, ch. 9.

[6] D. S. Wulfman, "Synthetic applications of diazonium ions," in *Diazonium and Diazo Groups: Part 1*, S. Patai Ed. New York: Diazonium and Diazo Groups: Part 1, 1978, ch. 16, pp. 247-339.

[7] E. Merino, "Synthesis of azobenzenes: the coloured pieces of molecular materials," *Chemical Society Reviews,* vol. 40, no. 7, pp. 3835-3853, 2011.

[8] G. E. Parris, "Environmental and metabolic transformations of primary aromatic amines and related compounds," New York, NY, 1980: Springer New York, in Residue Reviews, pp. 1-30.

[9] W. Al Zoubi, A. A. S. Al-Hamdani, S. D. Ahmed, and Y. G. Ko, "A new azo-Schiff base: Synthesis, characterization, biological activity and theoretical studies of its complexes," *Applied Organometallic Chemistry,* vol. 32, no. 1, p. e3895, 2018.

[10] Y. Teng *et al.*, "A Schiff-Base Modified Pt Nano-Catalyst for Highly Efficient Synthesis of Aromatic Azo Compounds," *Catalysts,* vol. 9, no. 4, p. 339, 2019.

[11] J. L. Pratihar, P. Mandal, C. K. Lai, and S. Chattopadhyay, "Tetradentate amido azo Schiff base Cu(II), Ni(II) and Pd(II) complexes: Synthesis, characterization, spectral properties, and applications to catalysis in C–C coupling and oxidation reaction," *Polyhedron,* vol. 161, pp. 317-324, 2019.

[12] R. Azadbakht, N. Chidan, S. Menati, and M. Koolivand, "A New Azo-Schiff Base Dual-mode Chemosensor: Colorimetric Detection of Cobalt Ions and Fluorometric Detection of Aluminum Ions in Aqueous Ethanol Solution," *Journal of Fluorescence,* vol. 33, no. 2, pp. 527-538, 2023.

[13] H. Nishihara, "Multi-Mode Molecular Switching Properties and Functions of Azo-Conjugated Metal Complexes," *Bulletin of the Chemical Society of Japan,* vol. 77, no. 3, pp. 407-428, 2004.

[14] H. Hessoon and F. Karam, "Synthesis, identification, biological activity and anti-cancer activity Studies of Hetrocyclic Ligand Azo-schiff Base with Au(III) Complex," *Egyptian Journal of Chemistry,* vol. 65, no. 1, pp. 327-334, 2022.

[15] K. F. Mohammed and H. A. Hasan, "Synthesis, Chemical and Biological Activity Studies of Azo-Schiff Base Ligand and Its Metal Complexes," *Chemical Methodologies,* vol. 6, no. 12, pp. 905-913, 2022.

[16] S. Kamali, M. Orojloo, R. Arabahmadi, and S. Amani, "Design and synthesis of a novel azo-Schiff base ligand: Its application as a colorimetric chemosensor for selective detection of Ni2+ and CN– in aqueous-organic media, computational studies, antimicrobial properties, and molecular logic circuits," *Journal of Photochemistry and Photobiology A: Chemistry,* vol. 433, p. 114136, 2022.

[17] Ö. Özdemir, "Bis-azo-linkage Schiff bases—Part(II): Synthesis, characterization, photoluminescence and DPPH radical scavenging properties of their novel luminescent mononuclear Zn(II) complexes," *Journal of Photochemistry and Photobiology A: Chemistry,* vol. 392, p. 112356, 2020.

[18] S. Bal and J. D. Connolly, "Synthesis, characterization, thermal and catalytic properties of a novel carbazole derived Azo ligand and its metal complexes," *Arabian Journal of Chemistry,* vol. 10, no. 6, pp. 761-768, 2017.

[19] B. R. Kirthan, M. C. Prabhakara, H. S. Bhojya naik, R. Viswanath, and P. H. Amith Nayak, "Optoelectronic, photocatalytic and biological studies of mixed ligand Cd(II) complex and its fabricated CdO nanoparticles," *Journal of Molecular Structure,* vol. 1244, p. 130917, 2021.

[20] P. Štarha and R. Křikavová, "Platinum(IV) and platinum(II) anticancer complexes with biologically active releasable ligands," *Coordination Chemistry Reviews,* vol. 501, p. 215578, 2024.

[21] T. Q. Manhee and A. J. Alabdali, "Synthesis, characterization and anticancer activity of Ni(II), Cu(II), Pd(II) and Au(III) complexes derived from novel Mannich base," *Vietnam Journal of Chemistry,* vol. 62, no. 2, pp. 201-210, 2024.

[22] Z. M. Abdnoor and A. J. Alabdali, "Synthesis, characterization, and anticancer activity of some azole-heterocyclic complexes with gold(III), palladium(II), nickel(II), and copper(II) metal ions," *Journal of the Chinese Chemical Society,* vol. 66, no. 11, pp. 1474-1483, 2019.

[23] B. Musikavanhu, Y. Liang, Z. Xue, L. Feng, and L. Zhao, "Strategies for Improving Selectivity and Sensitivity of Schiff Base Fluorescent Chemosensors for Toxic and Heavy Metals," *Molecules,* vol. 28, no. 19, p. 6960, 2023.

[24] I. Vogel, *Practical organic chemistry*, 5th ed. United Kingdom: Person Education, 2011, p. 1552.

[25] S. Shibata, M. Furukawa, and R. Nakashima, "Syntheses of azo dyes containing 4,5-diphenylimidazole and their evaluation as analytical reagents," *Analytica Chimica Acta,* vol. 81, no. 1, pp. 131-141, 1976.

[26] M. Hashemi, Z. Solati, A. Ghodsi, and S. Ahmadian, "Azo-substituted Schiff base complex of Pt(II): Synthesis, characterization, DFT and TD-DFT study," *Synthetic Metals,* vol. 210, no. Part B, p. 398-403, 2015.

[27] K. R. Balinge and P. R. Bhagat, "A polymer-supported salen-palladium complex as a heterogeneous catalyst for the Mizoroki-Heck cross-coupling reaction," *Inorganica Chimica Acta,* vol. 495, p. 119017, 2019.

[28] M. Chegeni, A. Molseghi, M. Mehri, S. Dehdashtian, and H. Nasr Esfahani, "Fabrication of gum Arabic with red mud as a photobiocomposite for antibacterial activity," *Journal of Photochemistry and Photobiology A: Chemistry,* vol. 448, p. 115302, 2024.

[29] G. Miliauskas, T. A. van Beek, P. R. Venskutonis, J. P. H. Linssen, P. de Waard, and E. J. Sudhölter, "Antioxidant activity of Potentilla fruticosa," *Journal of the Science of Food and Agriculture,* vol. 84, no. 15, pp. 2004.

[30] D. J. Hashim and S. M. Mahdi, "Preparation, Characterization, and Biological Study of New Halogenated Azo-Schiff Base Ligands and Their Complexes," *Journal of Medicinal and Chemical Sciences,* vol. 6, no. 7, pp. 1555-1576, 2022.

[31] C. Anitha, C. D. Sheela, P. Tharmaraj, and R. Shanmugakala, "Studies on Synthesis and Spectral Characterization of Some Transition Metal Complexes of Azo-Azomethine Derivative of Diaminomaleonitrile," *International Journal of Inorganic Chemistry,* vol. 2013, no. 1, p. 436275, 2013.

[32] K. Nakamoto, Infrared and Raman Spectra of Inorganic and Coordination Compounds, Part B: Applications in Coordination, Organometallic, and Bioinorganic Chemistry, 6th ed. Hoboken, NJ, USA: Wiley and Sons Ltd, 2009.

[33] D. L. Pavia, G. M. Lampman, G. S. Kriz, and J. R. Vyvyan, *Introduction to spectroscopy*, 5th ed. India: Cengage India, 2015, p. 784.

[34] S. M. Mahdi, "Preparation, Charecterazation of new nitro-chalcone azo ligands and their divalent ionic complexes," J. Phys. Conf. Ser., vol. 1294, no. 5, p. 052036, Sep. 2019.

[35] M. Balci, Basic ^{1}H- and ^{13}C-NMR Spectroscopy. Amsterdam, Netherlands: Elsevier Science, 2005.

[36] M. S. Refat, E.-D. I. M., A. Z. M., and S. El-Ghol, "Spectroscopic studies and biological evaluation of some transition metal complexes of Schiff-base ligands derived from 5-arylazo-salicylaldehyde and thiosemicarbazide," *Journal of Coordination Chemistry,* vol. 62, no. 10, pp. 1709-1718, 2009.

[37] N. Uspenski and S. Konobejewski, "Die Beugung der Röntgenstrahlen in mikrokristallinischen Strukturen," *Zeitschrift fuer Physik,* vol. 16, no. 1, pp. 215-227, 1923.

[38] J. D. Hanawalt, H. W. Rinn, and L. K. Frevel, "Chemical Analysis by X-Ray Diffraction: Classification and Use of X-Ray Diffraction Patterns," *Powder Diffraction,* vol. 1, no. 2, pp. 2-14, 1986.

[39] T. J. Al-Hasani and Z. S. Almaliky, "New Pd and Pt Complexes of Guanine –Azo Dye: Structural, Spectroscopic, Dyeing Performance and Antibacterial Activity Studies," *Iraqi Journal of Science,* vol. 56, no. 4A, pp. 2718-2731, 2023.

[40] V. Bondet, W. Brand-Williams, and C. Berset, "Kinetics and Mechanisms of Antioxidant Activity using the DPPH.Free Radical Method," *LWT - Food Science and Technology,* vol. 30, no. 6, pp. 609-615, 1997.

[41] J. Zou, L. Zhu, X. Jiang, Y. Wang, Y. Wang, and X. Wang, "Curcumin increases breast cancer cell sensitivity to cisplatin by decreasing FEN1 expression," (in eng), *Oncotarget,* vol. 9, no. 13, pp. 11268-11278, 2018.